

UNCLASSIFIED

AD NUMBER
AD487875
NEW LIMITATION CHANGE
TO Approved for public release, distribution unlimited
FROM Distribution authorized to U.S. Gov't. agencies and their contractors; Administrative/Operational Use; 16 MAR 1966. Other requests shall be referred to Office of Naval Research, Arlington, VA 22203.
AUTHORITY
ONR ltr 16 Feb 1979

THIS PAGE IS UNCLASSIFIED

AD No. \_\_\_\_\_

**UNCLASSIFIED**

487875



NAVSO P-970

REPRINTED FROM

U.S. NAVY JOURNAL of

**UNDERWATER ACOUSTICS**

Volume 16, No 3

July 1966

D D C  
RECORDED  
AUG 31 1966  
D

This document is subject to special export controls, and each transmittal to foreign governments or foreign nationals may be made only with prior approval of Office of Naval Research (Code 468), Washington, D.C. 20360.

**UNCLASSIFIED**

## **DISCLAIMER NOTICE**

**THIS DOCUMENT IS BEST QUALITY PRACTICABLE. THE COPY FURNISHED TO DTIC CONTAINED A SIGNIFICANT NUMBER OF PAGES WHICH DO NOT REPRODUCE LEGIBLY.**

When this article is referenced in unclassified reports or articles or listed in unclassified bibliographies (except TAB), indexes, etc., the citation should give the author and title followed by: In "Unpublished Report," Office of Naval Research, Code 468, and date (month and year) of the particular issue involved.

UNCLASSIFIED

## APPLICATION OF THE NEAR-FIELD-ARRAY TECHNIQUE TO SONAR EVALUATION

W. James Trott and Ivor D. Groves

U.S. Navy Underwater Sound Reference Laboratory  
Orlando, Florida 32806

(Received 16 March 1966)

### ABSTRACT

The design, construction, and step-by-step tests of the near-field array as it has been developed at the Underwater Sound Reference Laboratory are described. The optimum design and design tolerances for several arrays have been found by means of a digital computer. A guide for estimating the cost of an array for application to a particular sonar evaluation is derived from experience in the construction of these new arrays.

### INTRODUCTION

Fifteen years ago, sonar evaluation measurements were comparatively simple. Space requirements could be satisfied by a test distance of 10 feet and a water depth of 20 feet. To make conventional far-field measurements on present-day sonar transducers, however, great distances and tremendous volumes of water are required. For example, to evaluate a BQS-6 sonar transducer at frequencies up to 6 kHz, a test distance of 350 feet and a water depth greater than 130 feet would be required. These large test distances bring new problems — ambient noise, inhomogeneities that refract and scatter the transmitted signal, and uncertainty in bearing determination when transducers are suspended deep enough to distinguish direct from surface-reflected transmission.

The theory of sonar calibration in the far field, or Fraunhofer zone, is well known. In the far field, the wave impedance is resistive and quantities measured at one radial distance are related by the law of spherical spreading to those at a greater distance in the same direction.

The problems caused by large distances can be eliminated if the measurements are made close to the transducer in the near field or Fresnel zone, but the results must be expressible in terms of the far field. The usefulness of existing calibration facilities, which is very limited for far-field measurements on large transducers, can be extended greatly, if near-field measurements can be used. In theory, however, the near-field measurements are quite complex in contrast to the fairly simple conventional far-field ones.

Within the near field of a directional sound source, the wave impedance can be highly reactive; the pressure and particle velocity may vary widely from point to point — they may even be in phase quadrature at many points. In contrast to far-field measurement procedure, a simple point-by-point determination of sound pressure in the near field is not sufficient. The sound pressure at one radial distance is not related to that at a greater distance in the same direction by the law of spherical spreading.

Mathematically and experimentally, the complex near sound field can be treated as a superposition of plane waves traveling outward in all directions. That is to say that data obtained within the Fresnel zone by integrating or averaging values measured over plane apertures can be related directly to values measured point-by-point in the Fraunhofer zone of the

sound field. Techniques have been developed at the Defense Research Laboratory, The University of Texas, for probe measurements over a plane aperture and over closed surfaces surrounding a source within its Fresnel zone.<sup>1-3</sup> Others have treated the problem in a similar manner.<sup>4</sup>

Suppose we consider first the sonar transducer as a receiver instead of as a source of sound. The transducer's characteristics are then expressed in terms of its sensitivity to the pressure in a plane, free-field sound wave traveling in a specified direction. We can construct a measuring array that will produce a plane-wave, free-field sound pressure throughout the volume occupied by the sonar transducer, even though the measured transducer and the measuring array are very close together. These are the essential features of the near-field-array technique. By reciprocity, the characteristics of the transducer as a source can be determined at these close distances by using the array as a receiver.

This paper presents the design and construction of the near-field array as it has been developed at the Underwater Sound Reference Laboratory. The optimum design and design tolerances for several arrays have been found by means of a digital computer. Construction details and step-by-step tests are described. From experience in constructing these new arrays, a cost estimate can be made on a proposed array for application to a particular sonar evaluation. The theory leading up to the array technique has been presented in earlier papers.<sup>5,6</sup>

#### THE SHADING FUNCTION

The near field of a directional sound source can be treated mathematically as a superposition of plane waves, or as the superposition of a plane wave and a diffracted wave. A circular piston source can be considered as producing a plane wave plus a wave, due to diffraction, emanating from the edge of the piston. Interference between these two waves produces the highly reactive and widely varying Fresnel-zone sound field so well described by Stenzel.<sup>7</sup>

The sound pressure  $p$  on the axis of a circular piston source is derived from

$$p = (i\rho c/\lambda) e^{i\omega t} \int_0^R u_0(1/r) e^{-ikr} ds, \quad (1)$$

where  $\rho c$  is the plane wave impedance,  $\lambda$  is the wavelength of the sound,  $u_0$  is the velocity amplitude of the piston,  $\omega$  is angular frequency,  $k = 2\pi/\lambda$ , and  $r$  is the distance to the position point of  $p$  on the axis of the beam from the surface element  $ds = 2\pi r dr$ . If the position point is at distance  $x$  along the beam axis and the radius of the piston is  $R$ , then (Ref. 7, Eq. (110))

$$\int_0^R (1/r) e^{-ikr} ds = (-2\pi/ik) [\exp\{-ik(R^2 + x^2)^{1/2}\} - e^{-ikx}]$$

and

<sup>1</sup>C. W. Horton and G. S. Innis, Jr., "The Computation of Far-Field Radiation Patterns from Measurements Made Near the Source," *J. Acoust. Soc. Am.* **33**, 877-880 (1961).

<sup>2</sup>C. W. Horton, "The Prediction of Far-Field Radiation Patterns from Measurements Made Near the Source," *JUA(USN)* **14**, 511-516 (1964) (Confidential).

<sup>3</sup>D. D. Baker, "Computation of Far-Field Characteristics from Near-Field Measurements," *JUA(USN)* **14**, 525-547 (1964) (Confidential).

<sup>4</sup>"Special Features -- Near-Field Studies," *JUA(USN)* **14**, 497-588 (1964) (Confidential) (Seven articles devoted to near-field calibration studies).

<sup>5</sup>W. J. Trott, "A Conventional Transducer Calibration Unconventionally Close," *JUA(USN)* **14**, 101-114 (1964) (Confidential).

<sup>6</sup>W. J. Trott, "Underwater Sound Transducer Calibration from Nearfield Data," *J. Acoust. Soc. Am.* **36**, 1557-1568 (1964).

<sup>7</sup>H. Stenzel, *Leitfaden zur Berechnung von Schallvorgängen* (Julius Springer, Berlin, 1939), part 2, section 4.

$$p = \rho c u_0 \{ \exp[i(\omega t - kx)] - \exp[i(\omega t - k(R^2 + x^2)^{1/2})] \}. \quad (2)$$

Equation (2) shows that the sound pressure amplitude on the axis of a circular piston source is due to a plane progressive wave (the first term) modulated by a second wave delayed by the distance to the edge of the piston. Thus, for this simple case, the sound field of the source can be treated mathematically as the superposition of a plane progressive wave and a diffracted wave emanating from the edge at the surface of the piston source. If we can eliminate modulation of the direct wave by the diffracted wave within the Fresnel zone, then we will have the required measuring transducer — one that produces a plane-wave, free-field sound pressure throughout the volume occupied by the sonar transducer when the two transducers are close together. Absence of the pressure undulations normally produced by the interference of these two waves should be an indication that the goal has been achieved.

The array must be acoustically transparent so that standing waves do not develop between it and any transducer to be measured, and so that it will not alter the normal radiation impedance load on the measured transducer. Transparency is achieved by constructing the array of many piezoelectric transducers, each small with respect to the wavelength, widely spaced, and operating well below resonance. The elements of the array, operating well below resonance, will be unaffected by changes in the radiation load caused by the presence of the measured transducer. If the impedance of the individual elements is equal to or greater than the  $\rho c$  of the medium, then the average admittance of the array will be equal to the admittance of the medium, and the array will be transparent. Shading — reducing the source strength of the peripheral elements — eliminates the diffracted wave.

Consider the measuring array in the  $y, z$  plane, the origin at the center of the array, and radiation in the direction of  $x$ . If the diffracted wave is eliminated and only a plane wave of finite extent exists in nearby  $y, z$  planes, then, within the near field, the sound pressure function  $p(x, y, z)$  must be equal to  $|p(y, z)|e^{i(\omega t - kx)}$  and the magnitude  $|p(y, z)|$  must be the same function as the velocity shading function  $u(y, z)$ . This relationship could be used in a series of simultaneous equations to derive the shading function for the array of point sources. A radial Gaussian shading function  $\exp(-ar^2)$  is of this type, but is unacceptable because it does not produce a constant-pressure region of sufficient extent for near-field measurements.

The radiation impedance of a piston source is reactive at low frequencies and approaches  $\rho c$  loading as the diameter of the piston source becomes one wavelength or more. It seems logical that the dimensions of the array must be equal to or greater than a wavelength before a plane wave is produced; likewise, the extent of the shaded area must be about one wavelength in order to eliminate the diffracted wave. The depth of the plane-wave region along the  $x$  axis will increase with increasing frequency. This is in agreement with the experimental data.

#### THE SHADING FUNCTION

As stated in the original papers,<sup>5,6</sup> the shading function is based on a line array of elements whose source strengths are shaded from the center out in proportion to the coefficients of the binomial probability distribution for  $r$  occurrences in  $n$  independent trials when the probability in any single trial is  $1/2$ . This fact makes it convenient to find the shading coefficients in tables.<sup>8</sup>

The basic unit to which this line shading function is applied is a line array of equally spaced elements whose source strengths are proportioned to the coefficients of a binomial series having the power  $n$ . The unit is replicated  $n$  times with a center-to-center spacing equal to the element spacing  $d$ . Like the Gaussian shading function, the basic unit does not produce a constant-pressure region for near-field measurements, but, by replication, the resultant shading function<sup>8</sup> does. The far-field directional response of such a line array in the plane of the line is given by

<sup>8</sup>National Bureau of Standards, Applied Mathematics Series No. 6, Tables of the Binomial Probability Distribution (U.S. Government Printing Office, Washington, D.C., 1950).

$$p(\theta) = [(\sin n\phi)/(n \sin \phi)] \cos^n \phi, \quad (3)$$

where  $\phi = (\pi d/\lambda) \sin \theta$ ,  $d$  is the element spacing,  $\lambda$  is the wavelength, and  $\theta$  is the angle in the plane of the line between the normal to the line and the direction of observation.

In deriving a suitable shading function, unshaded elements are added to or deleted from the center of the line array, depending on the value of  $n$ . When this is done, Eq. (3) is modified to

$$p(\theta) = [(\sin m\phi)/(m \sin \phi)] \cos^n \phi, \quad (4)$$

where  $(m - n)$  is the number of unshaded elements added to the center of the line array. If  $m$  in Eq. (4) remains fixed and  $n$  increases without limit, the expression approaches a Gaussian pattern. A plane array shading function is obtained by means of the second product theorem.<sup>5,6,9</sup> This shading produces approximately circular symmetry and at the same time simplifies design and construction of the array, as is shown later in this paper.

#### COMPUTED SOUND FIELD

From the information in the original papers,<sup>5,6</sup> Hanish of the Naval Research Laboratory selected a shading function for a 2500-element plane array suitable for measurements on the BQS-6 sonar. He devised a Fortran program for the IBM 7094 computer to determine sound pressure and phase over planes parallel to the array at several distances along the  $x$  axis from the origin at the center of the array. For every element position  $(y, z)$  in the array, there is a computed value for the pressure and its phase relative to that of the source velocity in each plane at positions  $x$ .

Hanish<sup>10</sup> shows that a shading function represented by  $m = 36$ ,  $n = 26$  produces, close to the array, a plane wave throughout a volume sufficient to contain the BQS-6 for measurements at frequencies from 1 to 6 kHz. The element spacing in this array is 8 inches, or 0.8 wavelength at 6 kHz. The phase remains constant over the measuring region, but the calculations indicate a spherical wave at the periphery with as much as 100-degree phase delay from a plane wave at  $x = 7\text{-}1/2$  wavelengths at 3 kHz and 20 wavelengths at 6 kHz. At 1 kHz, the sound pressure across the region of measurement shows some undulations. Above 6 kHz, where the element spacing exceeds 0.8 wavelength, the sound field no longer is suitable for measurements, as is shown by the computations for 9 and 12 kHz.<sup>10</sup>

Upon review of these data, a new shading function  $m = 37$ ,  $n = 49$  was recommended by the first author. This function represents a line shading for 50 elements in the values of 0.00468, 0.0145, 0.0378, 0.0843, 0.164, 0.279, 0.423, 0.578, 0.721, 0.837, 0.916, 0.962, 0.986, 0.995, 0.999, 20 elements 1.000, 0.999, 0.995, 0.986, 0.962, 0.916, 0.837, 0.721, 0.578, 0.423, 0.279, 0.164, 0.0843, 0.0378, 0.0145, 0.00468. With permission of S. Hanish, the computed sound pressure and phase for his plane array based on this line shading is shown in Table I for one quadrant of the planes along  $x$ . The  $x$  axis is at the lower right corner of each tabulation. The phase is quite stable over the area in the  $xy$  plane equal to the area of the array and is equal to the plane-wave phase due to an array of point sources  $(kx + (1/2)\pi)$ . The computed sound pressure and phase variation for  $x = 125$  cm at 1 kHz and for  $x = 325$  cm at 3 kHz agree with  $x = 750$  cm at 6 kHz, thus proving a  $1/\lambda$  relationship along  $x$  (Eq. (1)). The maximum variation in sound pressure and phase appears along the diagonal of any square aperture along the  $x$  axis. This acceptable variation is the result of trying, for simplicity and economy, to achieve circular symmetry by means of the second product theorem, which produces circular symmetry only for a line shading that is Gaussian.<sup>9</sup>

<sup>9</sup>NDRC, Summary Technical Report of Division 6, Vol. 13, "The Design and Construction of Magnetostriction Transducers," Section 5.5.3 (1946).

<sup>10</sup>S. Hanish, M. A. Blizard, and R. A. Matzner, "Design of a Plane-Wave, Near-Field Calibration Array," Naval Research Laboratory Memorandum Report No. 1565 (2 Sept. 1964).

TABLE I. Computer Data for One Quadrant of a Plane Array Showing Pressure Amplitude and Phase in Planes at Distance  $x$  from and Parallel to the Array

6	8	10	13	17	20	24	28	32	36	40	44	47	49	50	51	51	50	49	49	48	48	48	48	47
8	10	13	17	22	26	31	37	42	47	52	57	60	63	65	66	66	65	64	63	63	63	63	63	63
10	13	17	22	28	34	41	47	54	61	67	73	77	81	83	84	84	84	83	82	81	81	81	81	81
13	17	22	28	35	43	51	60	69	77	85	92	98	103	106	107	107	106	105	104	103	103	103	103	103
17	22	28	35	44	54	64	75	86	96	106	114	122	127	131	133	133	132	131	129	128	128	128	128	128
20	26	34	43	54	66	78	91	104	117	129	139	148	155	160	162	162	161	159	158	157	156	156	157	157
24	31	41	51	64	78	93	109	125	140	154	166	177	185	190	193	193	192	190	188	187	186	186	187	187
28	37	47	60	75	91	109	127	146	163	179	194	206	216	222	225	225	224	222	220	218	218	218	218	219
32	42	54	69	86	104	125	144	164	184	205	222	236	246	253	257	258	256	254	251	250	249	249	249	250
36	47	61	77	96	117	140	163	186	209	230	248	264	276	284	288	289	287	284	282	280	279	279	279	280
40	52	67	85	106	129	154	179	205	230	253	273	291	304	313	317	318	316	313	310	308	307	307	307	308
44	57	73	92	114	139	166	194	222	248	273	296	316	329	338	343	344	342	338	335	333	332	332	332	332
47	60	77	98	122	148	177	206	236	264	291	316	334	349	360	365	366	363	360	356	354	353	353	353	353
49	63	81	103	127	155	185	216	246	276	304	329	349	365	376	381	382	380	376	373	370	369	369	369	369
50	65	83	106	131	160	190	222	253	284	313	338	360	376	387	392	393	391	387	383	381	379	379	380	380
51	66	84	107	133	162	193	225	257	288	317	343	365	381	392	398	399	396	392	388	384	384	384	384	384
51	66	84	107	133	162	193	225	258	289	318	344	366	382	393	399	399	397	393	389	386	385	385	386	386
50	65	84	106	132	161	192	224	256	287	316	342	363	380	391	396	397	394	390	386	384	382	383	383	384
49	64	83	105	131	159	190	222	254	284	313	338	360	376	387	392	393	390	386	382	380	379	379	380	380
49	63	82	104	129	158	188	220	251	282	310	335	356	373	383	388	389	386	382	378	376	375	375	376	377
48	63	81	103	128	157	187	218	250	280	308	333	354	370	381	386	386	384	380	376	373	372	373	373	374
48	63	81	103	128	156	186	218	249	279	307	332	353	369	379	384	385	382	379	375	372	371	372	372	373
48	63	81	103	128	156	186	218	249	279	307	332	353	369	379	384	385	383	379	375	373	372	372	372	373
48	63	81	103	128	156	187	218	249	279	307	332	353	369	380	385	386	383	380	376	373	372	372	373	374
49	63	81	103	128	157	187	219	250	280	308	332	353	369	380	386	386	384	380	377	374	373	373	374	374

(a) Pressure amplitude, NRL square array, 1 kHz,  $x = 1.667\lambda$  (250 cm)

101	84	70	57	47	38	32	27	25	23	23	23	23	27	28	30	31	33	33	34	34	33	32	31
84	68	53	41	31	23	16	12	9	8	8	9	10	11	13	14	16	17	18	18	18	17	16	16
70	53	39	27	17	9	3	-1	-3	-4	-5	-6	-6	-3	-1	0	1	2	3	4	4	4	3	2
57	41	27	15	5	-1	-8	-12	-14	-14	-14	-15	-14	-13	-11	-10	-8	-7	-6	-6	-6	-7	-8	-8
47	31	17	5	-3	-11	-17	-21	-24	-25	-25	-25	-23	-22	-21	-19	-18	-17	-16	-16	-16	-16	-17	-17
38	23	9	-1	-11	-19	-24	-29	-31	-32	-33	-32	-31	-30	-28	-27	-25	-24	-24	-23	-23	-24	-24	-25
32	16	3	-8	-17	-24	-30	-34	-37	-38	-38	-38	-37	-35	-34	-32	-31	-30	-29	-29	-29	-30	-30	-30
27	12	-1	-12	-21	-29	-34	-38	-41	-42	-42	-42	-41	-39	-38	-37	-35	-34	-33	-33	-33	-34	-34	-34
25	9	-3	-14	-24	-31	-37	-41	-43	-43	-43	-43	-42	-40	-39	-38	-37	-36	-36	-36	-36	-36	-37	-37
23	8	-5	-16	-25	-32	-38	-42	-45	-46	-46	-46	-45	-43	-42	-40	-39	-38	-37	-37	-37	-37	-38	-38
23	8	-5	-16	-25	-31	-38	-42	-45	-46	-46	-46	-45	-43	-42	-41	-39	-38	-37	-37	-37	-37	-38	-38
24	9	-4	-15	-25	-32	-38	-42	-44	-45	-46	-46	-45	-43	-41	-40	-39	-38	-37	-36	-36	-37	-37	-38
25	10	-3	-14	-23	-31	-37	-41	-43	-44	-45	-45	-44	-42	-40	-39	-38	-36	-36	-35	-35	-36	-36	-37
27	11	-1	-13	-22	-30	-35	-39	-42	-43	-43	-43	-42	-40	-39	-38	-36	-35	-34	-34	-34	-34	-35	-35
28	13	0	-11	-21	-28	-34	-38	-40	-42	-42	-41	-40	-39	-38	-36	-35	-34	-33	-33	-33	-33	-34	-34
30	14	1	-10	-19	-27	-32	-37	-39	-40	-41	-40	-39	-38	-36	-35	-33	-32	-32	-31	-31	-31	-32	-32
31	14	2	-8	-18	-25	-31	-35	-38	-39	-39	-39	-38	-36	-35	-33	-32	-31	-30	-30	-30	-31	-31	-31
33	17	3	-7	-17	-24	-30	-34	-37	-38	-38	-38	-36	-35	-34	-32	-31	-30	-29	-29	-29	-29	-30	-30
33	18	4	-6	-16	-24	-29	-33	-36	-37	-37	-37	-36	-34	-33	-32	-30	-29	-28	-28	-28	-29	-29	-30
34	18	4	-6	-16	-23	-29	-33	-36	-37	-37	-36	-35	-34	-33	-31	-30	-29	-28	-28	-28	-28	-29	-29
34	18	4	-6	-16	-23	-29	-33	-36	-37	-37	-36	-35	-34	-33	-31	-30	-29	-28	-28	-28	-28	-29	-29
33	18	4	-6	-16	-23	-29	-33	-36	-37	-37	-37	-36	-34	-33	-31	-30	-29	-28	-28	-28	-28	-29	-29
32	17	3	-7	-16	-24	-30	-34	-36	-38	-38	-37	-36	-35	-33	-32	-31	-30	-29	-28	-28	-29	-29	-30
32	16	3	-8	-17	-24	-30	-34	-37	-38	-38	-38	-37	-35	-34	-32	-31	-30	-29	-29	-29	-29	-30	-30
31	14	2	-8	-17	-25	-30	-34	-37	-38	-38	-37	-36	-34	-33	-31	-30	-29	-29	-29	-29	-30	-30	-31

(b) Phase, NRL square array, 1 kHz,  $x = 1.667\lambda$  (250 cm)

TABLE I (continued)

0	1	2	4	5	7	9	12	14	16	17	18	19	19	19	19	20	20	20	19	19	20	20	20	19
1	4	6	10	14	18	24	30	36	39	43	46	48	48	49	49	49	50	49	49	49	49	50	49	49
2	6	9	15	21	28	36	46	53	59	64	68	71	72	73	73	74	74	74	74	74	74	74	74	74
4	10	15	24	34	48	63	79	92	102	111	118	123	125	126	126	127	128	128	127	127	128	128	128	127
5	14	21	30	41	57	79	111	129	143	155	166	172	175	176	177	179	179	179	178	178	179	180	179	178
7	18	28	40	57	81	117	146	170	189	205	219	227	231	233	234	236	237	236	236	236	236	237	236	236
9	24	36	51	72	101	134	172	210	248	287	298	304	306	308	310	311	310	309	310	311	311	310	310	310
12	30	46	67	101	146	192	239	278	309	336	357	372	378	381	384	386	387	386	386	386	387	387	387	386
14	36	53	77	109	150	203	258	324	360	391	416	432	440	443	447	450	451	450	449	449	450	451	450	449
16	39	59	87	123	169	230	300	360	400	435	463	481	489	493	496	500	501	500	499	499	500	501	500	499
17	43	64	95	135	187	254	336	391	435	472	502	522	531	535	539	543	544	543	542	542	543	544	543	542
18	46	68	101	146	201	287	357	416	463	502	535	556	566	570	574	578	579	578	577	577	578	579	578	577
19	48	71	103	148	207	298	372	432	481	522	556	578	588	593	597	601	602	601	599	600	601	602	601	600
19	48	72	105	150	210	304	378	440	489	531	566	598	598	603	607	611	613	611	610	610	612	613	612	610
19	49	73	106	152	213	306	381	443	493	535	570	593	603	607	612	616	617	616	614	615	616	617	616	615
19	49	73	106	152	213	308	384	447	496	539	574	597	607	612	616	620	621	620	619	619	621	621	620	619
20	49	74	107	154	216	310	386	450	500	543	578	601	611	616	620	624	624	624	623	623	625	626	625	623
20	50	74	108	156	219	311	387	451	501	544	579	602	613	617	621	626	627	626	624	625	627	628	626	625
20	49	74	108	156	219	310	386	450	500	543	578	601	611	616	620	624	626	625	623	623	625	626	625	623
19	49	74	107	156	219	309	386	449	499	542	577	599	610	614	619	623	624	623	621	622	624	624	623	622
19	49	74	107	156	219	310	386	449	499	542	577	600	610	615	619	623	625	623	622	622	624	624	623	622
20	49	74	108	157	220	311	387	451	501	544	579	602	613	617	621	626	627	625	624	624	626	627	626	624
20	49	74	108	157	220	311	387	451	501	544	579	602	613	617	621	626	627	625	624	624	626	627	626	624
20	49	74	108	157	220	310	386	450	500	543	578	601	612	616	620	625	626	625	623	624	626	626	625	624
19	49	74	107	156	219	310	386	449	499	542	577	600	610	615	619	623	625	623	622	622	624	624	623	622

(c) Pressure amplitude, NRL square array, 6 kHz, x = 2λ (50 cm)

84	85	93	97	94	93	93	92	92	93	93	93	92	93	93	93	93	92	93	93	93	93	92	93	93
85	85	90	92	89	90	90	89	89	89	90	89	89	89	90	90	89	89	89	90	90	89	89	89	90
93	90	92	94	91	92	92	91	91	91	92	91	91	91	92	92	91	91	91	92	92	91	91	91	92
97	92	94	94	92	92	92	91	91	91	92	91	91	91	92	92	91	91	91	92	92	92	92	91	92
94	89	91	92	89	90	90	89	88	89	89	89	89	89	90	90	89	89	89	90	90	89	89	90	
93	90	92	92	90	91	91	90	89	90	90	90	90	90	90	91	90	90	90	90	91	90	90	90	
93	90	92	92	90	91	91	90	89	90	90	90	90	90	91	90	90	90	90	91	90	90	90	91	
92	89	91	91	89	90	90	89	88	89	89	89	89	89	89	89	89	89	89	89	89	89	89	89	
92	89	91	91	88	89	89	88	88	88	88	88	88	88	88	88	88	88	88	88	88	88	88	88	
93	89	91	91	89	90	90	89	88	89	89	89	89	89	89	89	89	89	89	89	89	89	89	89	
93	90	92	92	89	90	90	89	89	89	90	90	89	89	90	90	89	89	90	90	90	89	89	90	
93	89	91	91	89	90	90	88	88	89	90	89	89	89	89	89	89	89	89	89	89	89	89	89	
92	89	91	91	89	90	90	88	88	89	89	89	89	89	89	89	89	89	89	89	89	89	89	89	
93	89	91	91	89	90	90	88	88	89	89	89	89	89	89	89	89	89	89	89	89	89	89	89	
93	90	92	92	90	91	91	90	89	89	90	90	89	89	90	90	89	89	90	90	90	89	89	90	
93	90	92	92	90	91	91	89	89	90	90	89	89	90	90	89	89	90	90	90	90	89	89	90	
93	89	91	92	89	90	90	88	88	89	90	89	89	89	89	89	89	89	89	89	89	89	89	89	
92	89	91	91	89	90	90	88	88	89	89	89	89	89	89	89	89	89	89	89	89	89	89	89	
93	89	91	91	89	90	90	88	88	89	89	89	89	89	89	89	89	89	89	89	89	89	89	89	
93	90	92	92	90	91	91	89	89	90	90	89	89	90	90	89	89	90	90	90	90	89	89	90	
93	89	91	92	89	90	90	88	88	89	90	89	89	89	89	89	89	89	89	89	89	89	89	89	
93	90	92	92	90	91	91	89	89	90	90	89	89	90	90	89	89	90	90	90	90	89	89	90	
93	89	91	92	89	90	90	88	88	89	90	89	89	89	89	89	89	89	89	89	89	89	89	89	
93	90	92	92	90	91	91	89	89	90	90	89	89	90	90	89	89	90	90	90	90	89	89	90	
93	89	91	92	89	90	90	88	88	89	90	89	89	89	89	89	89	89	89	89	89	89	89	89	
93	90	92	92	90	91	91	89	89	90	90	89	89	90	90	89	89	90	90	90	90	89	89	90	

(d) Phase, NRL square array, 6 kHz, x = 2λ (50 cm)

TABLE I (continued)

2	4	6	9	13	17	21	26	29	33	36	39	41	41	42	43	43	42	43	42	42	42	42	42	42
4	6	10	14	19	25	32	38	44	50	54	58	61	62	63	64	64	63	64	63	64	63	63	63	63
6	10	15	21	29	39	49	59	67	76	83	89	93	95	97	98	98	97	98	97	97	97	97	97	97
9	14	21	30	42	55	69	83	95	108	118	126	132	134	137	138	138	138	138	137	138	137	137	137	137
13	19	29	42	58	77	96	115	133	149	164	175	183	186	190	191	191	191	192	191	191	191	191	191	191
17	25	39	55	77	101	126	152	175	196	215	230	241	245	251	252	252	251	252	251	251	251	251	251	251
21	32	49	69	96	126	157	190	218	245	269	287	300	306	313	314	314	314	315	313	314	313	313	314	313
26	38	59	83	115	152	190	229	263	296	324	347	362	370	377	379	379	379	380	377	379	378	378	378	378
29	44	67	95	133	175	218	263	302	340	373	398	416	424	433	436	436	435	436	436	435	436	436	435	436
33	50	76	108	149	196	245	296	340	382	419	448	468	478	488	490	490	489	491	488	489	489	488	489	489
36	54	83	118	164	215	269	324	373	419	460	491	514	524	535	538	538	537	538	535	537	534	535	536	536
39	58	89	126	175	230	287	347	398	448	491	525	549	560	571	574	574	573	575	572	573	573	572	573	572
41	61	93	132	183	241	300	362	416	468	514	549	574	585	597	600	600	599	601	598	599	599	598	599	598
41	62	95	134	186	245	306	370	424	478	524	560	585	596	609	612	612	611	613	609	611	610	610	611	610
42	63	97	137	190	251	313	377	433	488	535	571	597	609	622	625	625	624	626	622	624	623	623	624	623
43	64	98	138	191	252	314	379	436	490	538	574	600	612	625	628	628	627	629	625	627	627	626	627	626
43	64	98	138	191	252	314	379	436	490	538	574	600	612	625	628	628	627	629	625	627	627	626	627	626
42	63	97	138	191	251	314	379	435	489	537	573	599	611	624	627	627	626	628	624	626	625	625	626	625
43	64	98	138	192	252	315	380	436	491	538	575	601	613	626	629	629	628	630	626	628	627	627	628	627
42	63	97	137	191	251	313	377	434	488	535	572	598	609	622	625	625	624	626	622	624	624	623	624	623
42	64	97	138	191	251	314	379	435	489	537	573	599	611	624	627	627	626	628	624	626	625	625	626	625
42	63	97	137	191	251	313	378	434	489	536	573	599	610	623	627	627	625	627	624	625	625	626	625	626
42	63	97	137	191	251	313	378	434	488	535	572	598	610	623	626	626	625	627	623	625	624	623	624	624
42	63	97	137	191	251	314	378	435	489	536	573	599	611	624	627	627	626	628	624	626	625	624	626	625
42	63	97	137	191	251	313	378	434	489	536	572	598	610	623	626	626	625	627	623	625	624	623	624	624

(e) Pressure amplitude, NRL square array, 6 kHz, x = 30λ (750 cm)

200	182	170	161	152	148	144	142	140	139	139	140	141	142	142	143	144	144	144	144	144	144	144	144
182	164	153	143	135	131	127	125	123	122	123	123	124	125	126	126	127	127	127	127	127	127	127	127
170	153	141	132	123	119	115	113	111	110	111	111	112	113	114	115	115	115	115	115	115	115	115	115
161	143	132	122	114	109	106	103	102	101	101	102	103	104	104	105	105	106	106	106	106	106	106	106
152	135	123	114	106	101	98	95	94	93	93	94	95	96	96	97	97	98	98	98	98	98	98	98
148	131	119	109	101	97	93	91	89	88	89	89	90	91	92	92	93	93	93	93	93	93	93	93
144	127	115	106	98	93	89	87	86	84	85	85	86	87	88	89	89	89	89	89	89	89	89	89
142	125	113	103	95	91	87	85	83	82	82	83	84	85	86	86	87	87	87	87	87	87	87	87
140	123	111	102	94	89	86	83	82	81	81	82	83	84	84	85	85	86	86	86	86	86	86	86
139	122	110	101	93	88	84	82	81	80	80	81	82	83	83	84	84	85	85	85	85	85	85	85
139	122	111	101	93	89	85	82	81	80	80	81	82	83	83	84	85	85	85	85	85	85	85	85
140	123	111	102	94	89	85	83	82	81	81	81	83	83	84	85	85	85	85	86	85	86	85	86
141	124	112	103	95	90	86	84	83	82	82	83	84	84	85	86	86	86	86	87	86	87	86	87
142	125	113	104	96	91	87	85	84	83	83	83	84	85	86	87	87	87	87	88	87	88	87	87
142	126	114	104	96	92	88	86	84	83	83	84	85	86	86	87	88	88	88	88	88	88	88	88
143	126	115	105	97	92	88	86	85	84	84	85	86	87	87	88	88	89	89	89	89	89	89	89
144	127	115	105	97	93	89	87	85	84	85	85	86	87	88	88	89	89	89	89	89	89	89	89
144	127	115	106	98	93	89	87	86	85	85	86	87	88	89	89	89	89	89	89	89	89	89	89
144	127	115	106	98	93	89	87	86	85	85	86	87	88	89	89	89	89	89	89	89	89	89	89
144	127	115	106	98	93	89	87	86	85	85	86	87	88	89	89	89	89	89	89	89	89	89	89
144	127	115	106	98	93	89	87	86	85	85	86	87	88	89	89	89	89	89	89	89	89	89	89
144	127	115	106	98	93	89	87	86	85	85	86	87	88	89	89	89	89	89	89	89	89	89	89
144	127	115	106	98	93	89	87	86	85	85	86	87	88	89	89	89	89	89	89	89	89	89	89
144	127	115	106	98	93	89	87	86	85	85	86	87	88	89	89	89	89	89	89	89	89	89	89

(f) Phase, NRL square array, 6 kHz, x = 30λ (750 cm)



TABLE I (continued)

5	6	7	8	9	11	12	14	15	17	19	20	22	23	24	25	26	27	27	27	27	26	25	25	25	
9	10	12	14	16	18	21	23	26	28	31	34	36	38	40	42	43	44	44	44	44	43	42	41	41	
10	18	20	23	27	30	34	38	43	47	52	56	60	64	67	70	72	73	74	74	73	72	70	69	68	
23	27	31	35	40	46	52	58	64	71	78	85	91	96	101	105	109	111	112	111	110	108	106	104	103	
33	38	44	50	57	63	70	78	82	91	101	111	120	129	137	144	149	154	157	159	158	156	153	150	147	146
44	52	59	68	78	88	100	112	124	136	150	162	174	185	194	202	208	212	214	213	211	207	203	199	197	
56	65	75	86	98	112	126	141	156	172	188	205	220	233	244	254	262	268	270	269	265	260	255	251	249	
67	78	90	103	117	134	151	169	187	206	226	245	263	279	293	305	314	321	324	322	318	312	306	301	298	
79	92	105	121	138	157	177	198	220	242	265	288	309	326	344	358	369	377	380	379	374	367	359	353	350	
90	104	120	137	157	178	201	225	249	274	301	327	351	372	390	406	418	427	431	429	425	416	407	401	397	
97	112	129	148	169	192	217	242	269	296	325	353	379	402	421	438	452	461	465	464	457	449	440	432	428	
103	119	137	157	179	204	230	257	285	315	345	374	402	426	447	465	479	489	493	492	485	476	467	459	455	
108	125	144	165	188	214	242	270	299	330	361	393	421	447	469	488	503	513	517	516	509	499	490	482	477	
110	127	146	167	191	218	245	274	304	332	367	399	426	454	476	495	511	521	526	524	517	507	497	489	484	
111	129	148	169	194	221	249	278	308	340	373	405	431	460	483	502	518	529	533	531	524	514	504	496	491	
113	130	149	171	196	223	251	281	311	343	376	409	439	465	498	507	523	534	539	537	530	520	509	501	496	
112	130	149	171	195	222	251	280	310	342	375	407	437	464	496	506	522	532	537	535	528	518	507	499	494	
112	130	149	171	196	223	251	281	311	343	376	409	439	465	498	507	523	534	539	537	530	520	509	501	496	
112	130	149	171	196	223	251	281	311	343	376	406	438	465	498	507	523	534	538	537	529	519	509	500	496	
112	130	149	171	195	222	251	280	310	342	375	407	437	464	496	506	521	532	537	535	528	518	508	499	495	
113	131	150	172	196	223	252	281	312	344	377	409	439	466	499	508	524	535	540	538	531	521	510	502	497	
112	129	149	170	195	222	250	280	310	342	374	407	437	463	496	505	521	531	536	534	527	517	507	498	494	
113	130	150	171	196	223	252	281	312	344	377	409	439	466	499	508	524	535	539	538	531	520	510	502	497	
112	130	149	171	195	222	251	280	311	342	375	408	438	464	497	506	522	533	537	535	528	518	508	500	495	

(i) Pressure amplitude, AUWE rectangular array, 2 kHz,  $x = 20.32\lambda$  (1524 cm, 50 ft)

-59	-70	-81	-89	263	256	281	246	263	241	240	239	239	240	241	243	245	246	248	249	251	252	252	253	253	
-77	-89	260	252	244	238	253	229	226	224	223	222	222	223	224	226	226	229	231	232	233	234	234	234	235	
-88	260	250	241	234	228	223	219	216	214	212	212	212	214	214	215	217	219	220	222	223	223	224	224	225	
266	253	244	235	228	222	216	212	209	207	206	205	205	206	207	209	211	212	214	215	216	217	218	218	218	
259	248	238	230	222	216	211	207	204	201	200	200	200	200	200	200	202	203	205	207	208	210	211	212	213	213
256	244	234	226	219	213	207	203	200	198	197	196	196	197	198	200	202	203	205	206	207	208	209	209	209	
254	242	232	224	217	211	205	201	198	196	195	194	194	195	196	198	200	201	203	204	205	206	207	207	207	
251	240	230	222	214	208	203	199	196	194	192	192	192	193	194	195	197	199	201	202	203	204	204	205	205	
250	238	228	220	213	207	201	197	194	192	191	190	190	191	192	194	196	197	199	200	201	202	203	203	203	
250	238	229	220	213	207	201	197	194	192	191	190	190	191	192	194	196	198	199	201	202	203	203	204	204	
250	239	229	221	213	207	202	198	195	193	191	191	191	191	192	194	196	198	199	201	202	203	203	204	204	
251	240	230	221	214	208	203	199	195	193	192	192	192	193	195	197	199	201	202	203	203	204	204	205	205	
252	241	231	222	215	209	203	199	196	194	193	192	192	193	194	196	198	200	201	202	203	204	205	205	206	
252	240	231	222	215	209	204	199	196	194	193	193	193	194	196	198	200	201	202	203	204	205	205	206	206	
253	241	231	223	216	210	204	200	197	195	194	193	193	194	195	197	199	200	202	203	204	205	206	206	206	
253	241	232	223	216	210	204	200	197	195	194	193	193	194	195	197	199	201	202	203	204	205	206	206	206	
253	241	232	223	216	210	204	200	197	195	194	193	193	194	195	197	199	201	202	203	204	205	206	206	206	
253	242	232	224	216	210	204	200	197	195	194	194	194	194	196	197	199	201	202	203	204	205	206	206	207	
253	241	232	223	216	210	204	200	197	195	194	193	193	194	195	197	199	201	202	203	204	205	206	206	206	
253	242	232	223	216	210	204	200	197	195	194	194	194	194	196	197	199	201	202	203	204	205	206	206	207	
253	242	232	223	216	210	204	200	197	195	194	194	194	194	196	197	199	201	202	203	204	205	206	206	207	
253	242	232	223	216	210	204	200	197	195	194	194	194	194	196	197	199	201	202	203	204	205	206	206	207	
253	242	232	223	216	210	204	200	197	195	194	194	194	194	196	197	199	201	202	203	204	205	206	206	207	
253	242	232	223	216	210	204	200	197	195	194	194	194	194	196	197	199	201	202	203	204	205	206	206	207	
253	242	232	223	216	210	204	200	197	195	194	194	194	194	196	197	199	201	202	203	204	205	206	206	207	
253	242	232	223	216	210	204	200	197	195	194	194	194	194	196	197	199	201	202	203	204	205	206	206	207	

(j) Phase, AUWE rectangular array, 2 kHz,  $x = 20.32\lambda$  (1524 cm, 50 ft)

On the basis of these computed sound fields, one can estimate the optimum shading function by selecting values of  $m$  and  $n$  for the new array such that the shading matches a plot of this shading function (the one that has produced the best sound field)  $m = 37$ ,  $n = 49$  versus position.

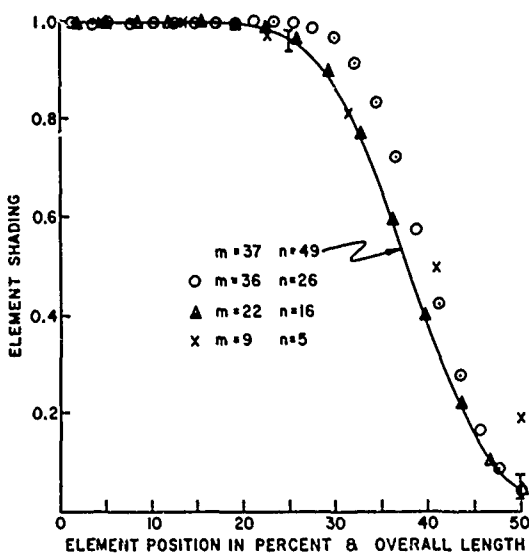


Fig. 1. Element shading as a function of overall length of line (0 percent is center of line)

Our experience indicates that the requirements for a measuring array are: (1) the dimensions of the array must be twice those of the transducer to be measured, (2) the number of elements required depends on the upper frequency limitation — that is, the number is determined by element spacing equal to or less than  $0.8$  wavelength, (3) the cutoff for the shading (the shading coefficient for the peripheral elements) should be about  $0.03$  to  $0.08$ , and (4) the source strength of the elements half way from the center to the edge should be between  $0.94$  and  $0.98$ .

Suppose it is desired to obtain measurements in an area  $12\lambda$  by  $12\lambda$  at the upper frequency limit. The number of spaces within the constant-pressure region will be  $12\lambda/0.8\lambda = 15$ . Figure 1 is a plot of the optimum shading function with the element positions shown in percentage of line length from the center. The shading function  $m = 22$ ,  $n = 16$  follows the curve very well and yields the 15 spaces in the region that has constant plane-wave pressure within  $1/2$  db. Thus a  $30 \times 30$ -element array  $m = 22$ ,  $n = 16$  is suitable for this measure-

ment. This conclusion is based on the computed data for  $m = 37$ ,  $n = 49$  in which the pressure amplitude function matched the shading function in the region extending out at least  $3\lambda$  lengths along the beam axis from the measuring array at the upper frequency limit. This was not the limit of useable sound field; the data computed for  $250$  cm and  $1$  kHz indicate that the limit of the near field for this  $30 \times 30$ -element array should extend out about  $60$  wavelengths at the upper frequency limit.

The shading function used in the published computations<sup>10</sup> is shown in Fig. 1 as circles designated as  $m = 36$ ,  $n = 26$ . It is seen that this shading exceeds the limits at the position half way from the center to the end of the line (the 25-percent point in Fig. 1). The computed sound field for this shading function was acceptable at the upper frequency limit out to  $x = 750$  cm but less desirable at the lower frequency limit, showing a spot  $+2.6$  db re average in the measuring region at  $x = 250$  cm at  $1$  kHz compared with  $0.5$  db at the same position and frequency for  $m = 37$ ,  $n = 49$ . The original near-field array built by USRL<sup>5,6</sup> was a  $12 \times 12$ -element array; the shading function for it is shown by the  $x$  marks designated  $m = 9$ ,  $n = 5$  on Fig. 1. Some variation in the sound field of this array was shown to be due to the cutoff at  $0.19$ .

The plane array need not be square, if the transducer to be measured produces a near field of rectangular cross section. In a special design requiring an array to produce a constant sound pressure over a volume  $10$  feet high,  $50$  feet wide, and  $50$  feet deep, the element spacing in the  $50 \times 50$ -element NRL array designed by Hanish was increased horizontally more than it was vertically. The horizontal spacing was increased from  $8$  to  $24$  inches and the vertical spacing was increased to  $9.6$  inches, producing a  $40 \times 100$ -foot array. Because of the  $24$ -inch spacing, the upper frequency limit for this array is  $2$  kHz. Computations, Table I, showed that this array would produce a plane-wave, constant-pressure sound field  $17\text{-}1/2$  feet high,  $50$  feet wide, and  $50$  feet deep, thus meeting the requirements. Additional elements can now be

fitted in along the shading curve to reduce the element spacing and raise the upper frequency limit of the array. This design was devised for the Admiralty Underwater Weapons Establishment.

#### DESIGN OF THE SECOND USRL ARRAY

Measurements made on the first USRL array consisting of 140 elements in a 12x12 array, corner elements left off, demonstrated that a uniform sound field is obtainable and that the design calling for capped piezoelectric ceramic cylinders is practical to construct. Another larger array consisting of 21 identical vertical lines has been designed and constructed. It is shaded to produce a plane array having approximately circular symmetry. Horizontal shading is achieved by connecting series capacitors to each individual line. The combination of identical shaded lines (shaded by means of the series capacitors), all lines and their capacitors connected in parallel, is the relationship referred to as the second product theorem in the original papers.<sup>5,6</sup>

Spacing between identical lines can be equal to the element spacing in the lines for the upper frequency limit ( $d = 0.8\lambda$ ). To cover a larger area at lower frequencies, the lines can be spaced further apart. Design data indicate that the constant-pressure region extends 5 feet of the 10-foot line length.

The 21-line array can be used to calibrate a 4x5-foot transducer at 10 kHz, a 5x5-foot one at 8 kHz, and a 14x5-foot one at 3.5 kHz. The lower frequency limit is about 1.5 kHz. Shading coefficients for this array have been carried to a lower value than the 0.19 used in the first array because the first one produced some undesired variations in the near sound field. These new lines are shaded down to the coefficient 0.047.

Each of the 21 individual lines of this array is composed of 26 PZT-4 capped tubes, 0.5-inch diameter x 0.5-inch long x 0.125-inch wall thickness. The elements are shaded in each line to the coefficients 0.047, 0.105, 0.202, 0.339, 0.500, 0.661, 0.798, 0.895, 0.953, 0.983, 1, 1, 1, 1, 1, 0.983, 0.953, 0.895, 0.798, 0.661, 0.500, 0.339, 0.202, 0.105, 0.047.<sup>11</sup> Element spacing is 4-1/2 inches center to center, resulting in a line 113 inches long. The elements are housed in a 10-foot length of 5/8-inch-I.D. x 0.063-inch-wall Teflon (FEP) transparent tubing. The inside of the tubing was etched for a length of 1 inch at each end for cementing to the metal termination seals.

Clear Teflon permits visual observation and easier removal of any trapped air bubbles. Earlier acoustic tests made on the Teflon tube had demonstrated it to be acoustically transparent in the frequency range of interest. Advantages of Teflon are its stiffness, which eliminates the need for a vacuum fixture when oil filling, and its low water permeability, which assures long life for the piezoelectric elements when the array is submerged in water.

A magnetic and electrostatic shield of 0.002-inch-thick Co-netic AA material is wrapped around the Teflon tubing over the 10-foot length to shield the transducer elements. The cable shield is electrically connected to this shield and is insulated from the water.

Tygon flexible tubing, type R-3603, with a 1-3/8-inch I.D. x 1/8-inch wall thickness provides the outside sheath that is in contact with the water. Both the Teflon and Tygon tubing are castor oil filled under vacuum to ensure removal of all air bubbles. The construction features are shown in Fig. 2.

Individual PZT-4 elements are capped on each end with a compression-type glass-to-metal seal cemented with Epon VI epoxy to form a hermetic seal. Before the element is capped, a small (0.005-inch-diameter) tinned copper wire extending out both ends is soldered to the inside electrode. A short length of 0.032-inch-diameter silver-plated phosphor-bronze

<sup>11</sup>The computations by Hanish were not available when this array was started, so the shading is more conservative than necessary and the measuring volume is reduced somewhat.

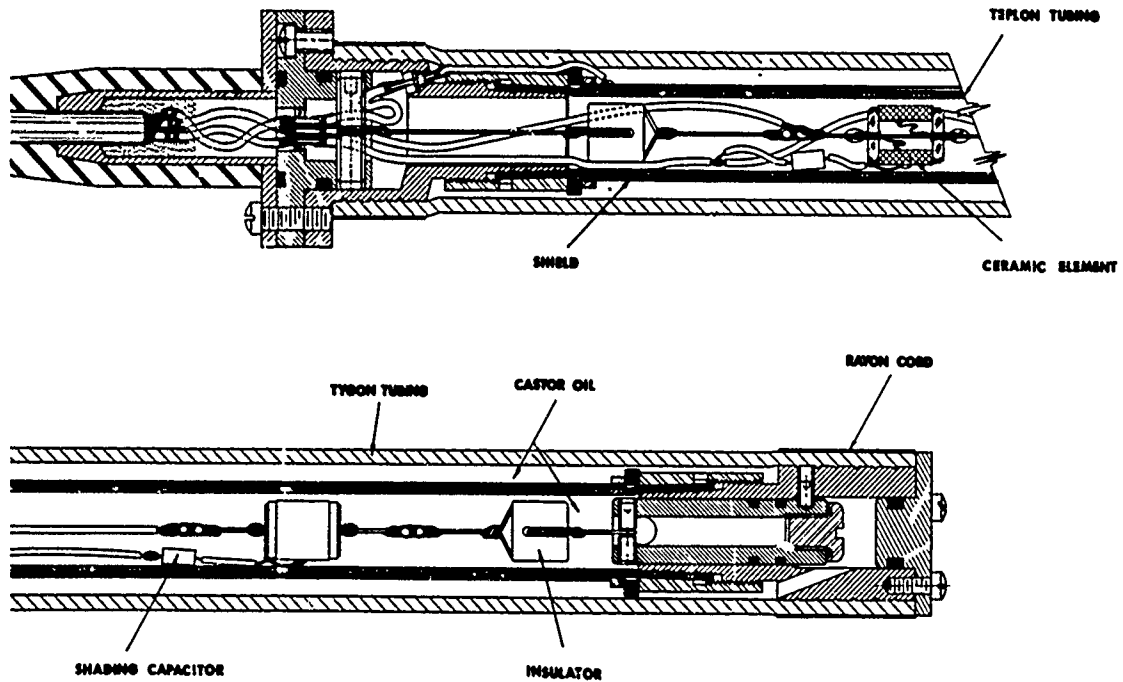


Fig. 2. Construction details of USRL line transducer type H33-10

wire passes through the central metal tube in each seal and is soldered in place to provide both a tension member and the electrical conductor for the inner electrode. These details are shown in Fig. 3. A typical element with the shading capacitor is shown in Fig. 4. These elements have been tested hydrostatically to 10,000 psi. They have been calibrated at 1000 psi; little or no change in sensitivity was observed.

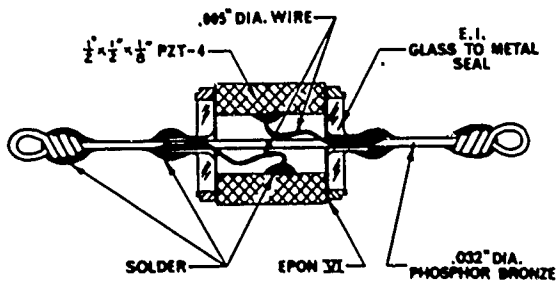


Fig. 3. Construction details of element type H33

Element shading was obtained by two methods. If the shading coefficient was 0.798 or larger, but less than 1, a portion of the outside silver electrode was removed by etching to reduce the capacitance and thus raise the impedance. Shading for all other elements was obtained by connecting a glass-sealed capacitor in series with the piezoelectric element. Capacitances ranged from 56 pF to 2200 pF. The average value of the capacitance for the unetched piezoelectric elements was 1150 pF.

Elements with the proper value of shading for the near-field array are selected by considering the product of the capacitance  $C$  and the measured open-

circuit sensitivity  $M$  of each element rather than the individual values of  $C$  and  $M$ . The unshaded elements at the center are selected so that the products  $MC$  are as close as possible to the same value. Since the elements are connected in parallel, the source strength per volt must be proportioned to the shading coefficients. Source strength is related to short-circuit receiving sensitivity, so the elements can be calibrated with a 1200-ohm resistor shunting the electrical output when the sensitivity is measured at about 500 Hz. The resonant frequency for the

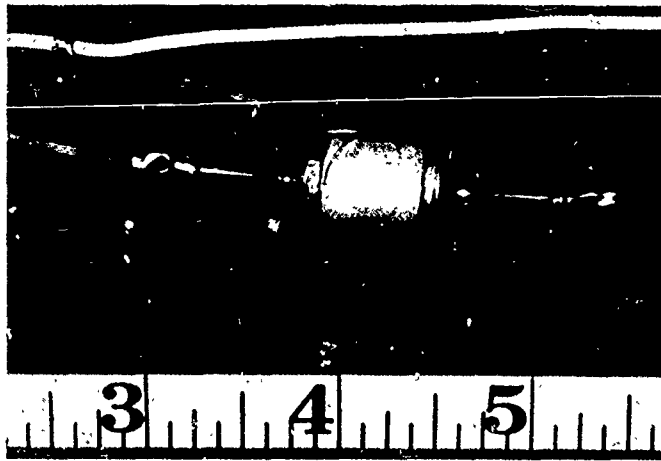


Fig. 4. Piezoelectric ceramic element with glass-sealed shading capacitor connected in series

principal vibrational mode of the element is above 70 kHz, well above the operational frequency range (1.5 to 10 kHz) of the array.

#### CALIBRATION AND SELECTION OF INDIVIDUAL ELEMENTS

Each piezoelectric capped tube was calibrated in a USRL type G19 calibrator<sup>12</sup> by comparison with a reference standard hydrophone. The test equipment, shown in Fig. 5, consists of a signal generator, a General Radio Model 1554A vibration and sound analyzer, a 40-db-gain low-noise transistor amplifier, a calibrated reference hydrophone, and the G19 calibrator. The calibrator was filled with peanut oil rather than water. This oil constitutes a medium of adequately high electrical resistivity in which to submerge the unprotected elements and their leads. The rubber diaphragm seal at the bottom of the calibrator deteriorates after prolonged exposure to peanut oil. Distilled water can and has been used when the elements are measured with the low-resistance shunt across the output. The dc resistance across the element was 50,000 ohms or higher when the element was submerged in distilled water and had negligible effect on the calibration. If a high-input-impedance amplifier is used, as at first, to measure the open-circuit voltage sensitivity, a medium of high resistivity is required.

After each element had been numbered and calibrated, the elements were arranged in groups according to sensitivity. Elements to have the shading coefficient 1.0 were chosen so that their sensitivities were within  $\pm 0.3$  db of each other. Elements to have the 0.983, 0.953, 0.895, and 0.798 coefficients were selected to provide the proper shading with respect to the average sensitivity of the unshaded elements. Random variations in the sensitivity, short-circuit current sensitivity, or the product  $MC$  of the piezoelectric ceramic elements due to manufacturing variables made it possible to choose most of the 0.983, 0.953, and 0.895-coefficient elements without removing part of the electrode. The sensitivities of these elements are lower by 0.2, 0.4, and 1.0 db than that of the unshaded elements. It was necessary to etch away a portion of the electrode for shading the elements to 0.798. The series capacitor values for the remaining elements were computed to give the proper voltage division for the desired shading when connected in series with a 1150-pF (average value) element.

<sup>12</sup>C. C. Sims, "Hydrophone Calibrator," USRL Research Report No. 60 (12 Apr. 1962) [AD-279 904].

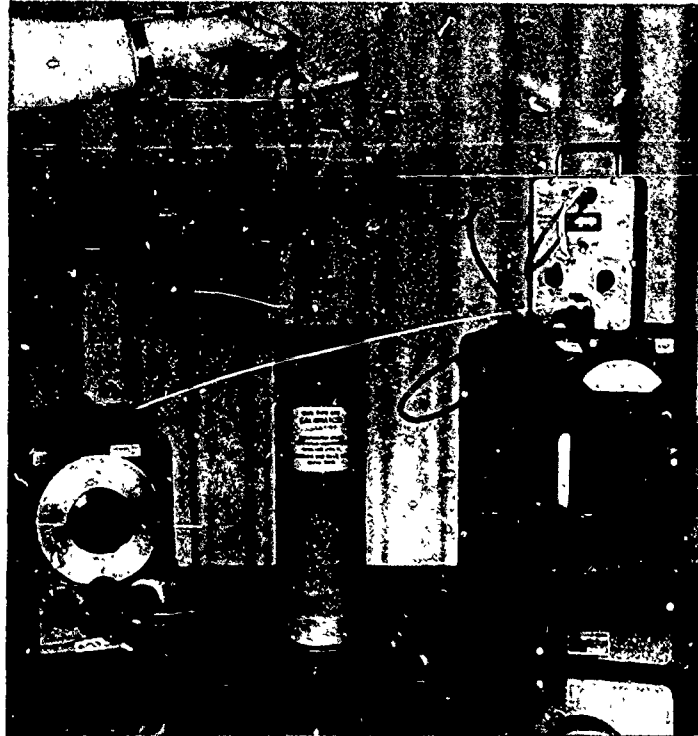


Fig. 5. Equipment used to calibrate each ceramic element at 400 Hz before assembly into line

Time and care in calibrating the elements is well spent. Assembly proceeds rapidly after the elements have been selected, and accurate initial measurements can save many hours of trouble shooting. Two separate calibrations on each element is recommended, with a third calibration recommended for any elements whose calibrations differ by more than 0.4 db. The average of the measured values should be used.

#### ASSEMBLY OF A LINE

Each line was assembled on a 14-foot board provided with nails separated by the element spacing  $d$ . The elements were held securely and accurately during assembly. Accurate positioning of the elements in the vertical line depends on the precision of this operation.

After the center wire was soldered to each of the elements, the second or ground lead was run the length of the line and soldered to the series capacitors and to the outside electrode of the unshaded elements. The capacitors had been soldered in place before the elements were placed on the board for assembly. The capacitors were soldered to the metal rim on the glass-to-metal seals and a small wire was soldered between the rim and the outer electrode for greater strength and to reduce the likelihood of pulling the electrode from the ceramic element. The wire that joins the capacitors to the outside electrode of the elements was installed with sufficient slack to permit some flexing and twisting of the line and thus reduce the chance of damage.

When all of the soldering had been completed, the solder joints and the elements were thoroughly cleaned by brushing with trichloroethane (inhibited methyl chloroform) to remove rosin and other residue. The dc resistance and capacitance across the assembled line were

UNCLASSIFIED

measured at the glass-to-metal seal in the top termination and recorded. If the capacitance differs greatly from the computed value, it is well to determine the cause of the discrepancy at this time. To help isolate a defective element, it was found convenient to separate the line at the center and compare capacitance measurements of the two halves. This procedure reduces the number of elements that require closer examination. The capacitance of the 21 lines was  $19,150 \text{ pF} \pm 250 \text{ pF}$ , which is a variation of less than  $\pm 1\frac{1}{2}$  percent. These values were obtained without cable, transducer shield, or castor oil.

An additional test was made to determine the correct voltage division on the elements shaded with series capacitors. A known voltage at 500 Hz was applied to the line input and the voltage across the elements was measured with a vacuum-tube voltmeter. The shading of 12 of 20 shaded elements could be checked quickly this way.

The line was then hung vertically, and the outside silver electrode of each ceramic element was coated with clear epoxy to minimize the loss of electroding material, which would change the element impedance. After the epoxy had hardened, the line was ready for installation in the Teflon tubing.

The cupro-nickel end fittings (shown in Figs. 6 and 7) are cemented to the Teflon tubing and retained by a compression band.

A wire attached to a screw in the oil filling hole in the metal termination was used to pull the 26-element line into the Teflon tube. The top and bottom of the tube were sealed with O-rings. Castor oil was applied to the bottom O-rings to assure easy seating without damage. The resistance and capacitance of the line were measured and recorded at the completion of each step in the assembly to ensure that any change that occurred during the preceding assembly operation would be detected and corrective action could be taken. After the top and bottom seals were secure, the line was ready for oil filling.

The stiff Teflon tube permitted oil filling under vacuum without the need for a vacuum fixture around the outside to prevent collapse of the tube. To fill the transducer, the line was

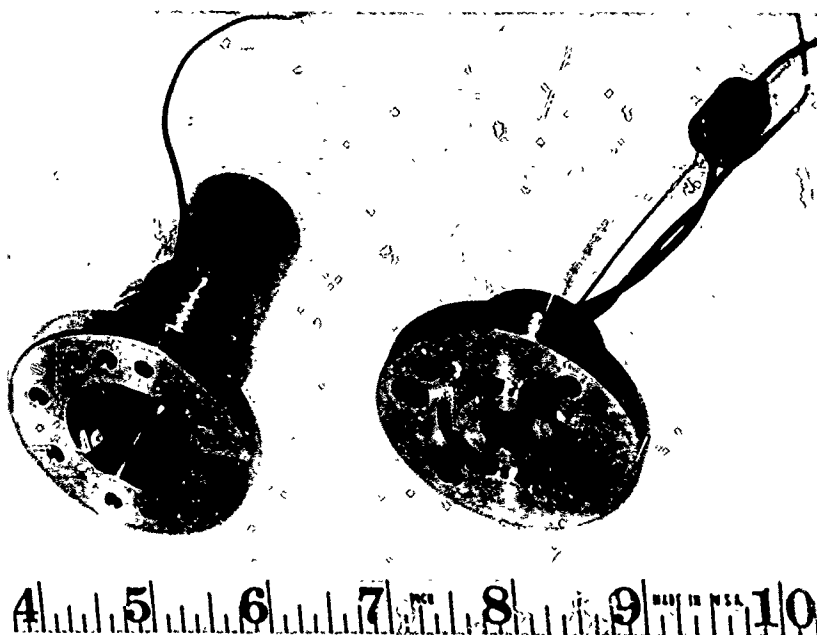


Fig. 6. Cupro-nickel top end fitting (left) and top line termination (right) showing glass-to-metal seal

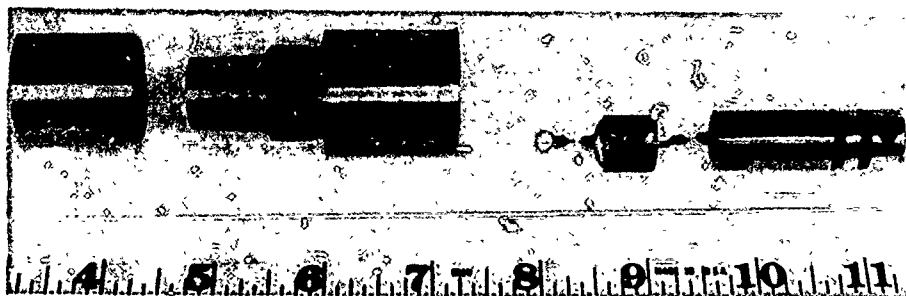


Fig. 7. Bottom end fitting with compression nut and line termination showing insulator and O-ring seals

placed in a position approximately 30 degrees from vertical with the line inverted to place the filling hole at the top. A vacuum hose from the oil-filling system was attached to the hole, and vacuum from a large mechanical pump was applied for at least 1 hour. Bakers DB-grade castor oil heated to 65°C was thoroughly degassed under vacuum (100 micron, 0.1 mm Hg) and then introduced at atmospheric pressure into the vacuum hose to the line transducer. The vacuum was again applied and the process repeated two to three times until no evidence of air bubbles remained. A small head of oil was kept on the line until the temperature stabilized to that of the room. The oil-seal plug was then inserted and tightened. Resistance and capacitance were measured at the glass-to-metal seal terminal, and the values were recorded.

The magnetic and electrostatic shield was wrapped around the outside of the Teflon and held in place by soldering several spots along its length. Insulating rings machined from Synthane grade XXXF were placed at the top and bottom to keep the shield from making electrical contact with the metal end fittings that are exposed to the water. The shield was connected electrically to the cable shield through a small wire to a glass-to-metal seal in the top end fitting (Fig. 6).

The outside Tygon tubing was slipped into place and each end sealed and secured to the end fittings by a tight wrap of rayon cord. The line transducer was then prepared for oil filling of this outer sheath.

The line was slipped into a 10-foot length of 1-5/8-inch I.D. pipe equipped with a short nipple for attachment to the vacuum line. The pipe was closed at one end and sealed to the line transducer at the other end. Vacuum was applied to both the vacuum fixture and the inside of the outer sheath. After at least 1 hour, the deaerated, heated castor oil was introduced in the Tygon boot to fill it completely. As with the inner tube, the vacuum was removed from both the transducer and the fixture when there was no further evidence of air bubbles. The transducer then was allowed to stand with a 2- to 3-inch head of oil until it cooled to room temperature. The seal plug was carefully installed to avoid trapping bubbles. The line transducer then was removed from the vacuum fixture and checked visually for air bubbles. Small bubbles can sometimes be maneuvered to the oil hole and removed without completely refilling under vacuum. Should a considerable number of air bubbles be found, it is best to drain all of the oil from the line and refill it under vacuum with heated oil of lower viscosity.

Each line was equipped with a 40-foot length of 0.350-inch neoprene-sheathed, two-conductor, shielded cable fitted with a molded gland that is sealed to the transducer by means of an O-ring. The cable shield was carefully insulated from the end fitting to prevent a water ground. The user thus has an option of grounding conditions so that he may find the condition that minimizes electrical coupling between the array and the measured transducer.

## BENCH TESTING THE ARRAY

The elements were carefully selected and spaced in their respective lines; however, a bench method was devised for testing the elements acoustically for proper shading after each line was completely assembled. A rubber cup was molded so that the lower portion would fit snugly around the Tygon sheath to form a watertight seal. The upper part of the cup is large enough to hold a 2-inch-O.D. x 1/2-inch-I.D. x 1/2-inch-long piezoelectric ceramic ring enclosed in polyurethane. The rubber cup and ceramic ring are shown in Fig. 8.



Fig. 8. Piezoelectric ceramic ring (left) and rubber cup (right) used in acoustic test of assembled line

The transducer line was hung from the ceiling in a vertical position. The cup and ceramic ring were slipped over the line at the bottom and then the cup was filled with water. The line was driven by a signal generator that produced 35 V at 15 kHz. The water-filled cup with the ceramic ring was positioned around each of the six unshaded center elements in the line and the output of the ring was amplified 20 db and measured with a vacuum-tube voltmeter or the sound and vibration analyzer. The values were recorded and averaged. The cup was then positioned around each of the shaded elements and the measured level with reference to the average of the unshaded element signals was compared to the computed value of the desired shading. Signal level dropped 30 db or more when the device was positioned between two adjacent elements. Later when the assembled plane array malfunctioned and, by substitution, the faulty line had been identified, this method of bench testing was used to locate the malfunctioning element.

## ACOUSTIC TESTS IN WATER

Each line transducer was calibrated separately. The near-field transmitting current response was measured with a standard hydrophone over the frequency range 500 Hz to 12 kHz. A single line produces a finite cylindrical wave of constant pressure amplitude in the near field along a line parallel to the line transducer and extending for half of its length at the mid-section. For cylindrical-wave spreading, the level diminishes by 3 db when the test distance is doubled. Direct comparison of the recorded data for these line transducers showed some variation in the response and some variation in the shape of the sound field — that is, the off-axis response. The average value of the line capacitance with 40 feet of cable was 20,300 pF. Series capacitors ranging from 0.00182  $\mu$ F to 0.620  $\mu$ F were used to produce the horizontal line shading.

The line transducers were now ready for final assembly into a plane array. The lines were connected in parallel with their series capacitors in the terminal strip shown in Fig. 9.

Rigging was constructed to facilitate positioning of a standard hydrophone directly in front of each line in the assembled array. The response of each line was ascertained in position by driving it alone shunted by a capacitor to simulate the impedance of the inactive lines. The driving source thus was presented with the same load while each line was tested. The value of the series capacitor was adjusted to correct the shading of each line to the correct value. The shading coefficients for the 21 lines, of course, are not the same as the 26 coefficients for the line elements.

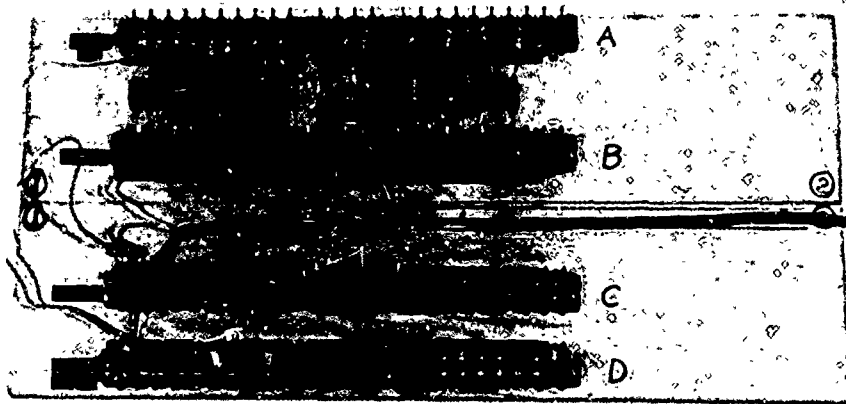


Fig. 9. Terminal strip with capacitors

The line transducers are hung from a horizontal 2-inch-diameter free-flooding pipe to form the complete array. An inverted U-shaped bracket positions and holds each line at the top. The U-bracket of each line is attached to a brass ring that slips over the pipe. This ring can be moved along the pipe to adjust the spacing between lines. The lower end of the line is held by a similar pipe-and-ring arrangement; however, a spring and turnbuckle are inserted at the end of each line to provide approximately 7 pounds of tension. To provide the tension on all the lines, it was necessary to weight the lower pipe. As a precautionary measure, tension-relief cables were installed to join the upper and lower pipes at the center of the array and at the extreme ends. These cables prevent excessive tension of the lines when starting and stopping vertical ascent or descent of the array. Particular attention was given to keeping the lines accurately positioned in the same vertical plane with the correct and constant spacing between them. A 19-line array with 4-1/2-inch line spacing is shown in Fig. 10.

Best calibration results can be obtained if the array is washed with a wetting agent and submerged 12 to 24 hours before making acoustic measurements. In this time, temperature stability is achieved, the lines become thoroughly wet, and any remaining air bubbles are absorbed or dislodged.

Troubleshooting the array can be difficult if the measured sound field varies considerably in the frequency range of interest. For this reason, the importance of bench tests has been emphasized. Two approaches can yield an answer to the problem. With a standard hydrophone mounted on the center axis in the near field, drive individually and alternately two lines in matching positions on each side of the center axis. Compare the responses of the two lines of each pair as the measurements are made progressively from the center to the extreme outside lines in the array. The level is affected by shading and cylindrical-wave distance loss, but each pair should yield identical response curves over the design frequency range. If two lines of such a pair do not produce the same curve, the nonconforming line must be identified. Sometimes the malfunctioning line can be identified without further measurements. At other times, it may be necessary to position the hydrophone in front of each line in question in the manner used to adjust the series capacitors to produce the design shading.

UNCLASSIFIED

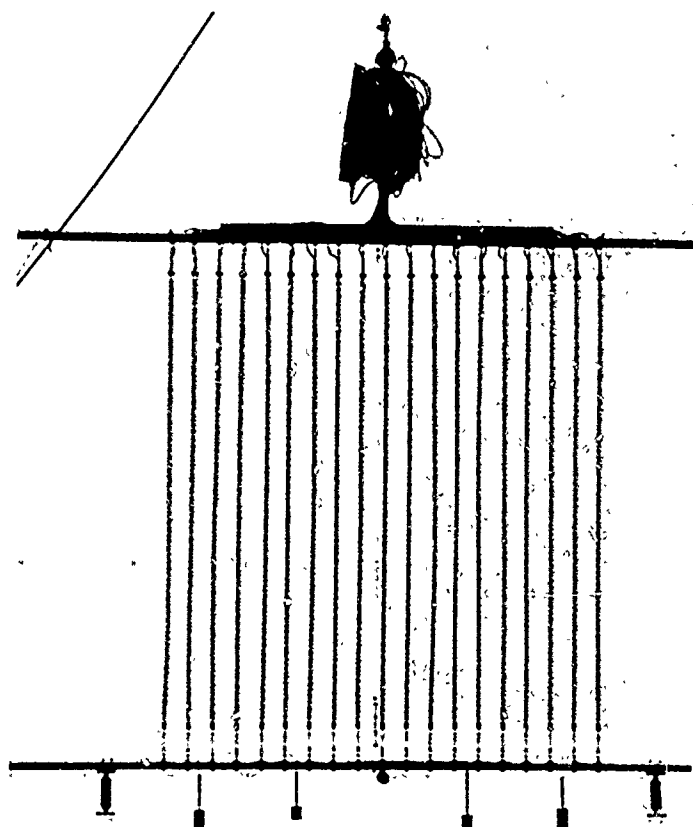


Fig. 10. Line array type H35-10 completely assembled — crossed wires in front and back of array help to position the lines

Should this procedure fail to provide conclusive results, an alternate method may be used. Position the receiving hydrophone on the center axis of the array in the near field. Drive the entire array and record the response versus frequency. Disconnect the line in question and measure the response of the array without this line. Return this line to the electrical circuit and drop the line on the other side of the center in its matching position. The line that produces the greatest variation in the sound field when connected to the circuit is generally the line with trouble. This line can be removed from the array and the individual elements again measured in the shop with the liquid-filled-ring technique previously described. A line that contains minor shading discrepancies can sometimes be switched to one of the extreme shaded positions and operate satisfactorily.

The sound field was explored primarily with two types of hydrophones. An LC32 transducer with an active element approximately 1-1/2 inches long was used as well as a USRL type F37 with an active length of 8 inches. The results of the measurements with these transducers were not significantly different. The response data were recorded from 500 Hz to 12 kHz at test distances 8, 16, 32, 64, and 128 inches along the acoustic axis and at 10, 20, and 30 inches above, below, and on each side of the acoustic axis. The sound field within the region to be used in near-field measurements was constant within  $\pm 1/2$  db, with a very few places showing as much as 1 db variation from the average sound pressure.

Tolerances in element shading and position have not been studied sufficiently to specify the design requirements. The near sound field of the first array was computed by the

Electro-Acoustic Systems Laboratory of Hazeltine Corp. The insertion of a maximum random error of 5 percent in element shading of a 14x14-element array showed no measurable change in the average deviation (0.05) of the normalized amplitude in the near-field sound pressure, and no measurable change in the average deviation ( $2^\circ$ ) of the phase of the pressure referred back to the surface of the array of point sources. From studies of the effect of element location errors upon directivity, it is our judgment that a position error of 2 percent of the element spacing  $d$  is permissible and can be achieved. In the first array, a 1/2-inch axial displacement of the center of the array from a plane did produce a measurable difference in the near sound field between the front and the back of the array at 12 kHz.

#### ALTERNATE SHADING METHODS

The same wall thickness need not be used for all of the elements. Wall thickness of the capped piezoelectric ceramic tubes can be varied to produce the required shading. This alternative eliminates the need for series capacitors, thus putting all outside electrodes of the elements at ground potential and reducing the shielding problem. The electrode can be etched to achieve the desired shading coefficient.

If the tubes are of the same diameter but of varying wall thickness, the thinner walled tubes will have not only higher capacitance, thus lower impedance, but the open-circuit voltage sensitivity of the thinner walled elements will be higher.<sup>13</sup> It is practical to vary the wall thickness from 0.030 to 0.125 inch for the same 1/2-inch O.D. and thus obtain 18 db of shading. The capacitance ratio will be 5:1 and the voltage sensitivity ratio approximately 1.58:1. Even greater variations are possible if the length of the tubes is changed also. The operational depth or hydrostatic pressure and the resonant frequency of the element will determine the minimum allowable wall thickness. The operational frequency range will also dictate the maximum dimensions of the elements from the standpoint of array transparency.

In large low-frequency arrays, flat disks or rectangular plates may be more practical than capped tubes. When several thousand elements are used to produce an array, the lower impedance of the tube elements is not required; the area of the element can be changed to provide the required shading. Likewise, the effective area and thus the impedance can be changed by cementing two or three plates together and connecting them electrically in parallel. A combination of different element dimensions and use of paralleled plates, with etched electrodes for close adjustment, can produce a more economical design.

#### APPLICATION

We have shown that the near field of the transducer can be resolved into a plane progressive wave and a diffracted wave. By suitable shading of the velocity or source strength of an element as a function of its distance from the center, it is possible to eliminate the interfering diffracted wave. The plane array thus produces a plane progressive wave of constant amplitude throughout a volume in its near field that is suitable for calibrating a transducer of dimensions

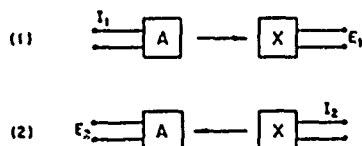


Fig. 11. Transducer arrangements for array calibration

less than half the dimensions of the measuring array. No other information about the measured transducer is required to determine from these near-field measurements the free-field voltage or current sensitivity, far-field transmitting current or voltage response, or far-field directivity of the unknown transducer.

Consider the array and the unknown transducers as constituting a system that is linear, passive, and reversible as shown in diagram form in Fig. 11. The near-field transmitting current response of the measuring array has been measured previously by probing the sound field with standard hydrophone; it is given by

<sup>13</sup>R. A. Langevin, "The Electro-Acoustic Sensitivity of Cylindrical Ceramic Tubes," J. Acoust. Soc. Am. 26, 421-427 (1954).

$$S_A = E_H/M_H I_A, \quad (5)$$

where  $S_A$  is the transmitting current response of the measuring array within the region for measurements;  $E_H$ ,  $M_H$  are the open-circuit voltage output and the free-field voltage sensitivity, respectively, of the standard hydrophone; and  $I_A$  is the current driving the array. So long as the pressure is the same over the region of the unknown transducer, its free-field voltage sensitivity is

$$M_X = E_X M_H / E_H. \quad (6)$$

In arrangement 1 of Fig. 11,

$$E_1/I_1 = S_A M_X.$$

If, as stated, the system is linear, passive, and reversible, then in arrangement 2

$$E_2/I_2 = E_1/I_1 = S_A M_X. \quad (7)$$

We want to determine the far-field transmitting current response of the unknown driven by current  $I_2$  when  $E_2$  is the open-circuit voltage output of the measuring array.

The ratio of the free-field voltage sensitivity to the far-field spherical-wave transmitting current response is equal to the spherical-wave reciprocity parameter  $J_s$ ,

$$M_X/S_X = J_s = 2D/\rho c,$$

where  $D$  is the reference distance for the far-field transmitting current response. In Eq. (7),

$$S_A M_X = S_A S_X J_s = E_2/I_2,$$

or

$$S_X = E_2/(I_2 S_A J_s),$$

and

$$S_X = (E_2/I_2)(\rho c/2D S_A). \quad (8)$$

Thus, with Eqs. (6) and (8), we can obtain the free-field receiving sensitivity and the far-field transmitting response from near-field measurements by using the techniques and calculations familiar to those experienced in far-field measurements.

Rotation of the unknown within the constant-amplitude plane-wave region will yield the free-field directivity of the unknown transducer in the same manner as it is obtained by rotation in the far field of a source, or when the receiver is in the far field of the measured transducer acting as a source for measuring the far-field directivity.

In measuring response and sensitivity of a line transducer or a single stave of a sonar transducer, the expense of constructing a plane array can be saved by using the equivalent of one line of this plane array. One shaded line will produce a cylindrical wave of constant amplitude over approximately half its length. The cylindrical wave pressure will diminish 3 db for twice the test distance, so distance must be measured.

Equation (6) can be used where a standard hydrophone measures the sound pressure in the region of the line. Equation (8) is modified to correct for distance loss. If the test distance is  $d$  and the reference distance for the far-field transmitting current response is  $D$ , then for the line or stave

$$S_X = (E_2/I_2)(d/D)^{1/2} (\rho c/2D S_A),$$

where  $S_L$  is now the near-field cylindrical-wave transmitting current response of the shaded line array at reference distance  $D$ , the same as the reference distance for the measured far-field transmitting current response  $S_x$  of the unknown.

Directivity of the unknown line cannot be measured in this cylindrical wave, but must be measured in the near field of a plane array.

To evaluate the BQS-6 sonar transducer by pulsed-sound far-field measurements, a test distance of 350 feet and a water depth of at least 130 feet are required. The transducer must be suspended to a depth of at least 65 feet to delay the surface-reflected sound pulse long enough for the direct measured sound to reach steady state. To evaluate the same transducer using the near-field measuring array, the sound pressure level is so low (less than -25 db) outside the near sound field of cross section equal to the area of the array that measurements can be made pulsed or continuous wave in water of depth less than twice the vertical dimension of the array. The horizontal dimensions of the water basin only need be sufficient to delay the boundary-reflected sound pulse long enough for the direct measured sound to reach steady state. The transducer and array can be suspended on a common frame. Short, stiff members will ensure accurate bearing determination.

The system of transducer and array is a reversible one, so, when the array is receiving, its sensitivity to surface- and bottom-reflected sound is also very low in relation to radiation along its beam axis. Refraction due to temperature gradients will have no effect on measurements at near-field test distances. Surface proximity may affect the radiation impedance of the sonar transducer, but this is a far less critical problem when the beam axis of a directional transducer is generally in the horizontal plane for evaluation. Of course the transducer and array system can be suspended from a cable and lowered to greater depths to measure the effect of hydrostatic pressure on the characteristics of the sonar transducer.

The array is ideal for measurements as a function of hydrostatic pressure and temperature in a closed tank. The near-field array technique makes possible the use of a spherical tank that maximizes the operating pressure for minimum wall stress. Such a tank has been designed for the Underwater Sound Reference Laboratory.

Since the test distance is not critical, the near-field array can be suspended over the side of a ship for sonar measurements in situ. If the array is twice the dimensions of the transducer and dome, then the measurements relate to the far-field of the sonar-dome system without the influence of the ship and water surface. Data can be compared to laboratory calibrations. If the array is larger and further away, then the near-field measurements can be related to far-field measurements made in situ. Thus the sonar-dome system, ship and surface environment, and propagation can be judged for their effects upon system performance.

Unlike other near-field measuring methods, where amplitude and phase must be determined point-by-point, the array technique can be used to measure radiated noise. Here the radiated noise must be predominantly from an area half the dimensions of the array for radiation in the direction of interest. For this measurement, the wavelength in Eq. (8) is the wavelength of the center frequency of a narrow band of noise and the radiated sound pressure given by Eq. (8) is  $S_x \frac{1}{2}$ .

A single near-field line array can be used in a small tank of water for production and repair quality-control measurements on sonar arrays. The near-field line array can be used to scan a surface other than a plane, thus reducing the data-acquisition time for probing methods of near-field measurements developed at other laboratories.

## CONCLUSIONS

Development and tests of the first plane array have been reported in earlier papers.<sup>5,6</sup> The second array, consisting of 21 line arrays each 10 feet long and consisting of 26 elements, is described in this paper. This design allows one to expand the area insonified at lower

UNCLASSIFIED

frequencies by spacing the lines further apart. This array can be used to calibrate the SQS-23 and the SQS-26 sonar.

A plane array has been designed and is under construction at the Underwater Sound Laboratory, New London, Connecticut, for measurements in a laboratory tank. A 34x34-foot plane array has been designed, analyzed by means of an IBM 7094 computer, and is under construction at the Naval Research Laboratory for installation at Lake Seneca in New York State. A 40 x 100-foot array has been designed and analyzed by means of an IBM 7094 computer by the Sound Division, Naval Research Laboratory, for the Admiralty Underwater Weapons Establishment at Portland, England. The Electro-Acoustic Systems Laboratory of Hazeltine Corp. is adapting the plane array theory to design and build under contract a cylindrical-surface phased array for testing the AN/AQS-10 helicopter sonar. Here at the Underwater Sound Reference Laboratory, we are designing a 30 x 30-element array to extend the usefulness of the 1000-pcf anechoic vessel for measurements under controlled temperature and hydrostatic pressure.

During construction of the 21-line array, a 30-minute, 16-mm color film was produced to demonstrate details of construction and testing. The film can be made available to those desiring to build a near-field measuring array.

#### Appendix

#### COST ESTIMATION

The cost of materials for an array constructed as described is approximately \$12 per element. This figure can be reduced by as much as 10 percent, if shading is accomplished without series capacitors. Another 10 percent can be saved in labor and material by using disks or slabs instead of capped cylinders. The 5/8-inch-I.D. Teflon tubing costs \$6 per foot. Other materials such as butyl rubber can be used in its place without sacrificing the low water permeability; however, butyl is not optically transparent and the oil could not be inspected visually for air bubbles. An accessory would also be required to prevent collapse of the tubing during oil filling under vacuum. The technique of oil filling could be practiced with transparent tubing until an air-free filling technique was assured.

The construction time for a large array like the 21-line array described requires 3 man-hours per element. The total cost of each 26-element line for materials and labor was \$624.